1,3-Diphospha-2-silaallylic Lithium Complexes and Anions: Synthesis, Crystal Structures, Reactivity, and Bonding Properties

Dirk Lange, Elke Klein, Holger Bender, Edgar Niecke,* Martin Nieger, and Rudolf Pietschnig

Institut für Anorganische Chemie der Universität Bonn, Gerhard-Domagk-Strasse 1, D-53121 Bonn, Germany

Wolfgang W. Schoeller*

Fakultät für Chemie der Universität Bielefeld, Universitätsstrasse, D-33615 Bielefeld, Germany

Henri Ranaivonjatovo

Laboratoire de Chimie de Coordination du CNRS, 205 route de Narbonne, F-31077 Toulouse-Cédex, France

Received September 8, 1997

Trichlorosilanes $RSiCl_3$ (R = t-Bu, Mes, Cp*, Is, OAr) reacted with a 4-fold excess of lithium phosphanide ArPHLi (Ar = 2,4,6-$^tBu_3C_6H_2$) to form 1,3-diphospha-2-silaallylic complexes **3a**−**f**. From the latter, the corresponding free allylic anions could be liberated by complexation of the lithium cation with [15]-crown-[5], as could be established on the basis of NMR spectra and X-ray structures. In addition, the bonding in the Li complexes was further investigated using ab initio calculations of double-ξ quality. The influence of cation solvation on the complex geometry was explored as well. The chemical reactivity of 1,3-diphospha-2-silaallylic anions with electrophiles (E = H^+, ClPR′R″) was investigated. 1,3-Diphospha-2-silapropenes **4a**−**d** and 1,3,4-triphospha-2-silabutenes-(1) **5a**−**e** and **6a** were prepared.

Introduction

In the past decades, a large variety of heteroallylic anions[1−3] and heteroalkenes[4−7] involving heavier main-group elements have been realized. Most of them are isolable due to either steric protection and/or stabilization by electronic effects of the (p−p)π system.[8,9] A challenge from the theoretical[10−12] as well as synthetic[2,3,13−18] point of view are π-systems containing both phosphorus and silicon. The first successful synthesis of a PSi π-system, corroborated by NMR spectroscopy, was reported by Smit and Bickelhaupt in 1984.[13] We published the first structural proof of a phosphasilene[17] (**5a**) as well as of a related delocalized 3p(π)-system, the lithium 1,3-diphospha-2-silaallylic complex **3a** (Schemes 1 and 2).[2] The latter congener may be compared to the allylic anions **A**,[19] **B**,[20] and **C**,[3] which were characterized by X-ray analysis as well (Scheme 3).

Here we report the synthesis of five other 1,3-diphospha-2-silaallyllithium complexes **3b**−**f** and the free anion **3a**′. The structures and reactions of these compounds to give phosphino- and diphosphinosilaphosphenes **4a**−**d**, **5a**−**e**, and **6a** are discussed in detail.

Results and Discussion

Synthesis. The lithium salts **3b**−**f** were obtained by treatment of 4 equiv of the lithium phosphide **1** with

(1) Jutzi, P.; Meyer, U. *Phosphorus Sulfur Relat. Elem.* **1988**, *40*, 275.
(2) Niecke, E.; Klein, E.; Nieger, M. *Angew. Chem., Int. Ed. Engl.* **1989**, *28*, 751.
(3) Driess, M.; Rell, S.; Pritzkow, H.; Janoschek, R. *Angew. Chem., Int. Ed. Engl.* **1997**, *36*, 1326.
(4) *Multiple Bonds and Low Coordination in Phosphorus Chemistry*; Regitz, M., Scherer, O. J., Eds.; Thieme: Stuttgart, 1990.
(5) Weber, L. *Chem. Rev.* **1992**, *92*, 1839.
(6) Okazaki, R.; West, R. *Adv. Organomet. Chem.* **1996**, *39*, 231.
(7) Driess, M. *Adv. Organomet. Chem.* **1996**, *39*, 193.
(8) Yoshifuji, M.; Shima, I.; Inamoto, N.; Hirotsu, K.; Huguchi, T. *J. Am. Chem. Soc.* **1981**, *103*, 4587.
(9) Güth, W.; Busch, T.; Schoeller, W. W.; Niecke, E.; Krebs, B.; Dartmann, M.; Rademacher, P. *New J. Chem.* **1989**, *13*, 309.
(10) Dykema, K. J.; Truong, T. N.; Gordon, M. *J. Am. Chem. Soc.* **1985**, *107*, 4535.
(11) Lee, J. G.; Boggs, J. E.; Cowley, A. H. *J. Chem. Soc., Chem. Commun.* **1985**, 773.
(12) Baboul, A. G.; Schlegel, H. B. *J. Am. Chem. Soc.* **1996**, *118*, 8444.
(13) Smit, C. N.; Bickelhaupt, F. *Tetrahedron Lett.* **1984**, *25*, 3011.
(14) Smit, C. N.; Bickelhaupt, F. *Organometallics* **1987**, *6*, 1156.
(15) van den Winkel, Y.; Bastiaans, H.; Bickelhaupt, F. *J. Organomet. Chem.* **1991**, *405*, 183.
(16) Driess, M.; Pritzkow, H.; Rell, S.; Winkler, U. *Organometallics* **1996**, *15*, 1845.
(17) Bender, H. R. G.; Niecke, E.; Nieger, M. *J. Am. Chem. Soc.* **1993**, *115*, 3314.
(18) Driess, M.; Rell, S.; Pritzkow, H. *J. Chem. Soc., Chem. Commun.* **1995**, 253.
(19) Gouygou, M.; Koenig, M.; Couret, C.; Escudié, J.; Huch, V.; Veith, M. *Phosphorus Sulfur Relat. Elem.* **1993**, *77*, 230.
(20) Underiner, G. E.; Tan, R. P.; Powell, D. R.; West, R. *J. Am. Chem. Soc.* **1991**, *113*, 8437.

S0276-7333(97)00793-0 CCC: $15.00
Publication on Web 05/13/1998

Scheme 1[a]

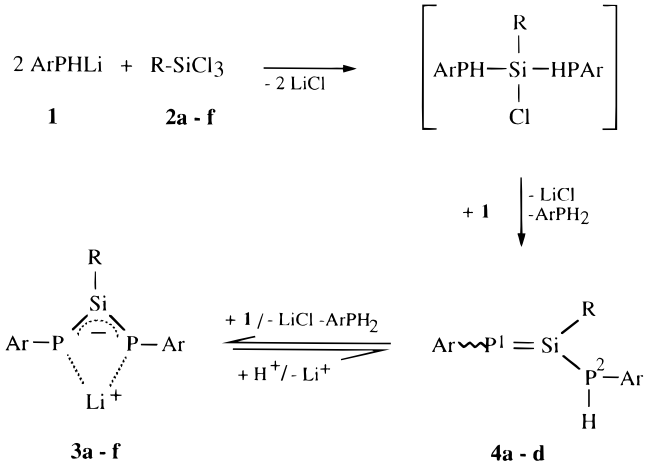

[a] **a**: R = ^{t}Bu. **b**: R = Mes. **c**: R = Cp*. **d**: R = Is. **e**: R = Ph. **f**: R = OAr (Ar = 2,4,6-^{t}Bu$_3$C$_6$H$_2$; Is = 2,4,6-^{i}Pr$_3$C$_6$H$_2$; Mes = 2,4,6-Me$_3$C$_6$H$_2$; Cp* = 1,2,3,4,5-Me$_5$C$_5$).

Scheme 2

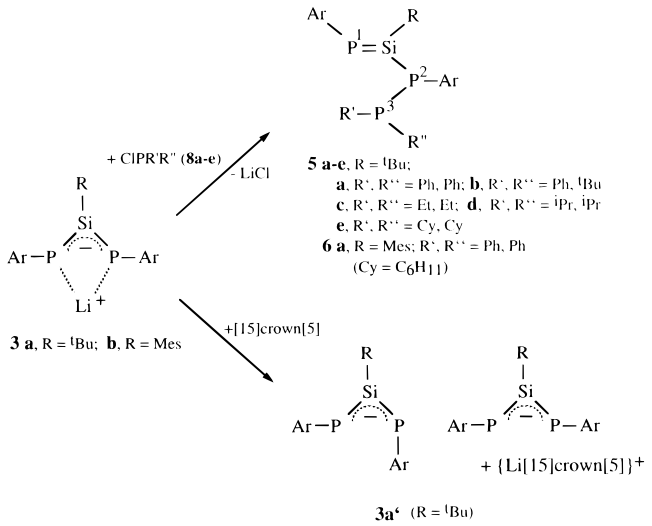

the corresponding trichlorosilanes **2b**−**f** in Et_2O or DME at −78 °C (Scheme 1, Table 1). This method is related to that used in the preparation of the 1,3-diphospha-2-silaallylic anion **3a**.[2] Solutions of these lithium salts are dark red and are extremely air and moisture sensitive; **3e** even decomposes when warmed over −30 °C. The compounds **3a**−**d** were isolated from a *n*-pentane/Et_2O or *n*-pentane/DME solution as dark red crystals. Addition of [15]-crown-[5] to a solution of **3a** in diethyl ether at room temperature gave the *E*/*Z* and *E*/*E* isomers of the free anion **3a′** (Scheme 2). Red-orange crystals of the *E*/*Z* isomer lithium crown etherate could be obtained by recrystallization from toluene.

Hydrolysis and Substitution Reactions. Hydrolysis of **3a**−**d** in Et_2O at 0 °C resulted in formation of the phosphinosilaphosphenes **4a**−**d**. Without attack at the double bond, one phosphorus atom was protonated (Table 2). The phosphinosilaphosphenes **4a**−**d** are thermally unstable and decompose when heated or treated with an excess of water. Therefore, we were unable to isolate them in pure form. In contrast, attack of softer electrophiles on **3a** and **3b**, such as, e.g., the chlorophosphines **8a**−**e**, yielded the phosphasilenes **5a**−**e** and **6a** (Table 3). However, only compound **5a** was sufficiently stable to allow its isolation from the reaction mixture.[17]

NMR Spectra. The ^{31}P chemical shift values for the allylic anions **3a**−**f** are collected in Table 1. They vary from −30 to −100 ppm depending on the substituent attached to the silicon atom. The symmetry of the complexes **3a**,**b**,**f**·2Et_2O is influenced by the solvent used and/or concentration. Thus, the ^{31}P NMR signal is split into four equidistant lines due to a $^1J_{PLi}$ coupling, and the ^{7}Li NMR signal appears as a triplet.[2] The high value of the $^1J_{PSi}$ coupling constant of **3a**, obtained from the ^{29}Si satellites (145.2 Hz), is indicative of the multiply bonded phosphorus atom,[13−15] while the high-field shift reflects the shielding effect of the negative charge on the P atoms.

An interesting effect was found in the ^{31}P NMR spectrum of compound **3a′**. At −30 °C, we observed a singlet (−22.3 ppm) with ^{29}Si satellites (183.1 Hz) for the *E*/*E* isomer and an AB system (−11.4 ppm/30.5 Hz, −19.1 ppm/30.5 Hz) with different $^1J_{PSi}$ coupling constants (234.8 Hz/173.7 Hz) for the *E*/*Z* isomer of the free allylic system. The coupling constant of 234.8 Hz is the largest value ever reported for $^1J_{PSi}$ in multiply bonded phosphorus−silicon compounds.[21]

Similar isomers of a related free anion have also been found for the corresponding triphosphaallylic−phosphorus system by Jutzi and Meyer,[1] revealing the same tendencies in the NMR data. The occurrence of a *Z*/*Z* compound is improbable because of the steric congestion due to the two Ar groups.

NMR data of **4a**−**d** are given in Table 2. The ^{31}P NMR spectra show the expected AX-systems with a downfield shift for the 2-fold-coordinated phosphorus atom and a signal at high field for the phosphino congener. For silaphosphene **4c**, the largest $^1J_{PSi}$ coupling constant for a neutral P═Si compound thus far was observed.

The ^{31}P NMR spectra of **5a**−**e** and **6a** show characteristic AMX patterns with the typical downfield shifts for the double-bonded phosphorus atoms. The $^3J_{PP}$ coupling constants of **5a** and **5e** are unusually large and probably indicate a P^1−P^3 through-space contact, which is corroborated for **5a** by its X-ray structure.[17] In comparison, **6a** shows a rather small value which evidences a different conformation of the P═Si−P−P skeleton.

Again, as in **4c** and **3a′**, the $^1J_{P=Si}$ coupling constants of **5a**−**e** are remarkably large and even the $^1J_{P-Si}$ couplings reach a value characteristic for a P═Si bond whereas all hitherto known $^1J_{P=Si}$ values are in the narrow range of 150−160 Hz.[13−15] This may be attributed to the electronic effect of the phosphino group attached to the silicon atom. The low coordination at the silicon atom is reflected by its deshielding, concomitant with a downfield shift of the ^{29}Si signal. A coupling to all three different phosphorus atoms is observed.

The geometrical parameters of the three structures **3a**−**c** differ only slightly depending on the substituent on the silicon atom and the complexing ether molecules. **3b** has exactly C_2 symmetry, while **3c** shows only a small distortion of bonds and angles due to the η^1-Cp*

(21) A remarkable exception is $LiP(SiH_3)_2$ showing a $^1J_{PSi}$ coupling constant of 256 Hz, see: Cradock, S.; Ebsworth, E. A. V.; Rankin, D. W. H.; Savage, W. J. *J. Chem. Soc., Dalton Trans.* **1976**, 1661.

Scheme 3

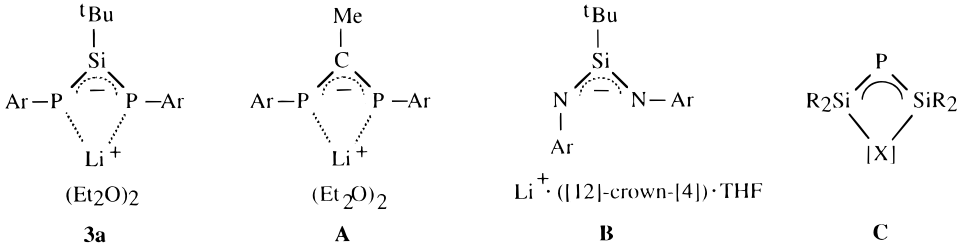

Scheme 4

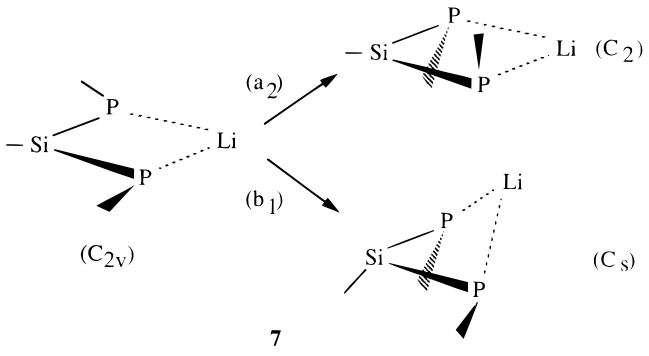

Table 1. ^{31}P NMR and ^{7}Li NMR Data of the Allylic Anions 3a−f

	R	^{31}P [ppm]	$^{2}J_{PP}$ [Hz]	^{7}Li [ppm]	$^{1}J_{PLi}$ [Hz]	$^{1}J_{PSi}$ [Hz]
3a[a]	tBu	−45.1 (q)		+2.66 (t)	46.5	145.2
3b	Mes	−33.3 (q)		−1.05 (t)	47.9	
3c	Cp*	−40.1 (s)		−2.55 (s)		
3d	Is	−31.0 (s)		−2.06 (s)		
3e	Ph	−51.8 (s)		−2.63 (s)		
3f	ArO	−99.7 (q)		−0.90 (t)	53.5	
3a′ (*E*/*E*)	tBu	−22.3 (s)				183.1
3a′ (*E*/*Z*)	tBu	(*E*)-19.1 (d)	30.5			173.7
		(*Z*)-11.4 (d)	30.5			234.8

[a] Reference 2.

Table 2. ^{31}P NMR and ^{29}Si NMR Data of 4a−d

	4a[a]	**4b**[b]	**4c**[c]	**4d**[d]
δP1 [ppm]	+142.0	+159.0	+169.2	+163.8
δP2 [ppm]	−125.0	−110.3	−124.0	−101.7
$^{2}J_{PP}$ [Hz]	6.0	14.6	22.9	15.3
$^{1}J_{PH}$ [Hz]	206.2	208.1	210.8	238.1
δSi [ppm]			+185.7	
$^{1}J_{P1Si}$ [Hz]	216.0		224.0	153.9
$^{1}J_{P2Si}$ [Hz]	95.2		79.2	134.8

[a] R = tBu. [b] R = Mes. [c] R = Cp*. [d] R = Is.

ligand on the silicon atom. All of them are σ-complexes, as indicated by an almost planar arrangement of the P−Si−P−Li skeleton. The most important bond lengths and angles are listed in Table 4, together with the corresponding values for the free anion **3a′**.

The P−Si bond lengths of the diphosphaallylic anions **3a**−**c** and **3a′** vary only slightly within a small range of 0.025 Å. Thus, they are characteristically shorter than a normal P−Si single bond distance of 2.25 Å[22] but only slightly longer than the P═Si double bond lengths found for phosphasilenes, e.g., as in **5a** (2.094(3) Å)[17] and the more recent examples (2.053(2), 2.062(1) Å).[3,18] The P−Si distance in the diphosphaallylic anions is

(22) Rademacher, P. Groesse und Gestalt von Molekülen. *Strukturen organischer Moleküle, Physikalische Organische Chemie*; Klessinger, M., Ed.; Verlag Chemie: Weinheim, 1987.

Table 3. ^{31}P NMR and ^{29}Si NMR Data of 5a−e and 6a

	5a[a]	**5b**[b]	**5c**[c]	**5d**[d]	**5e**[e]	**6a**[f]
δP1 [ppm]	+128.7	+122.1	+107.7	+121.9	+114.9	+157.7
δP2 [ppm]	−69.1	−75.8	−74.3	−75.7	−79.1	−48.8
δP3 [ppm]	−26.1	+29.3	−2.8	+29.6	+12.0	+0.2
$^{1}J_{P2P3}$ [Hz]	215.2	315.8	316.2	317.3	287.1	236.0
$^{2}J_{P1P2}$ [Hz]	23.9	38.7	42.9	39.1	34.8	44.1
$^{3}J_{P1P3}$ [Hz]	102.1	76.8	75.9	75.8	101.2	9.0
δSi [ppm]	+180.2	+185.9	+181.7	+186.0		
$^{1}J_{P1Si}$ [Hz]	203.0	208.3	200.8	206.9	207.4	197.0
$^{1}J_{P2Si}$ [Hz]	141.3	145.1	138.4	144.7	136.1	139.2
$^{2}J_{P3Si}$ [Hz]	13.1	13.2	4.9	11.5		

[a] R/PR′R″ = tBu/PPh$_2$. [b] R/PR′R″ = tBu/PPhtBu. [c] R/PR′R″ = tBu/PEt$_2$. [d] R/PR′R″ = tBu/P^{i}Pr$_2$. [e] R/PR′R″ = tBu/PCy$_2$. [f] R/PR′R″ = Mes/PPh$_2$.

Table 4. Important Bond Lengths (Å) and Angles (deg) of 3a−c and 3a′

	3a[a]	**3b**[b]	**3c**[c]	**3a′** [d]
Si1−P1	2.114(3)	2.123(2)	2.138(1)	(exo) 2.123(2)
Si1−P2	2.113(3)	2.123(2)	2.130(1)	(endo) 2.127(2)
P1−Li1	2.639(14)	2.562(11)	2.682(5)	
P2−Li1	2.670(13)	2.562(11)	2.637(6)	
Si1−C	1.915(7)	1.898(8)	1.946(3)	1.936(4)
P1−Si1−P2	104.9(1)	105.3(1)	103.0(1)	125.7(1)
Si1−P1−Li1	88.8(3)	86.1(2)	88.5(1)	
Si1−P2−Li1	88.0(3)	86.1(2)	89.9(1)	
C−P1−Si1	107.8(2)	107.7(2)	108.5(1)	105.2(1)
C−P2−Si1	108.4(2)	107.7(2)	115.8(1)	111.8(2)
P1−Si1−C	127.5(3)	127.3(1)	125.7(1)	128.6(2)
P2−Si1−C	127.6(3)	127.3(1)	131.3(1)	105.6(2)
P1−Li1−P2	78.3(3)	82.1(2)	77.8(2)	
P1−Si1−P2−Li1	0.1(0.3)	0.0(0.0)	7.7(0.1)	
C−P1−P2−C	75.5	83.0	101.8	184.1
Σ(Si1)	360.0	359.9	360.0	359.9

[a] Reference 2. R = tBu. [b] R = Mes. [c] R = Cp*. [d] R = tBu.

almost unaffected by the substituents, the interaction of the P atoms with the lithium cation, and the donor molecules (Et$_2$O, DME, [15]-crown-[5]). Noteworthy is the lack of a difference between the *E* (2.123(2) Å) and *Z* (2.127(2) Å) P−Si bond lengths within the same molecule **3a′**.

The P^1−Si^1−P^2 angle in the free anion is rather different from the corresponding angle in the lithium complexes. The complexation by lithium causes a decrease from 125.7(1)° (in **3a′**) to 104.9(1)° (in **3a**). The findings agree well with the results on the central angles at carbon (P−C−P 104.6°) in **A**[19] and nitrogen (N−Si−N 126.5(2)°) in **B**.[20]

Another peculiarity emerges from analysis of the projection of the anions along their P−P axis. In Figure 5 the structures of **3a** and **3a′** are compared with the lithium complex **A** and the free anion **B**.

The ideal allylic system is expected to be exactly planar. This is the case for the two free allylic systems

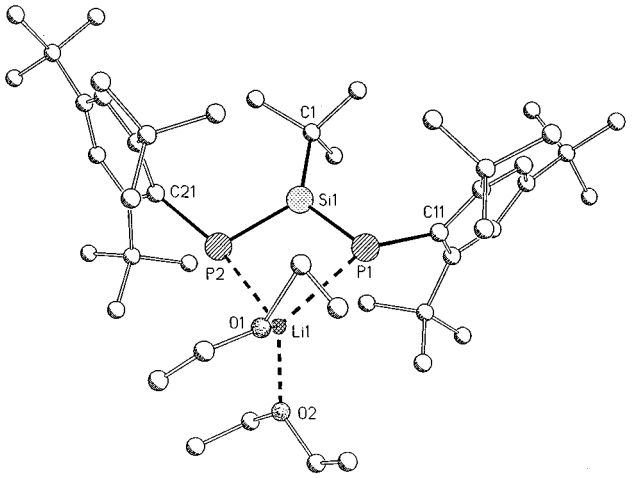

Figure 1. Molecular structure of the allylic complex **3a** ($2Et_2O$).[2]

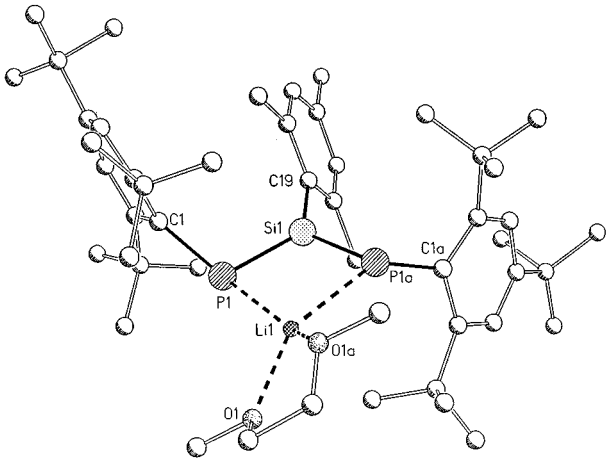

Figure 2. Molecular structure of the allylic complex **3b** (1DME).

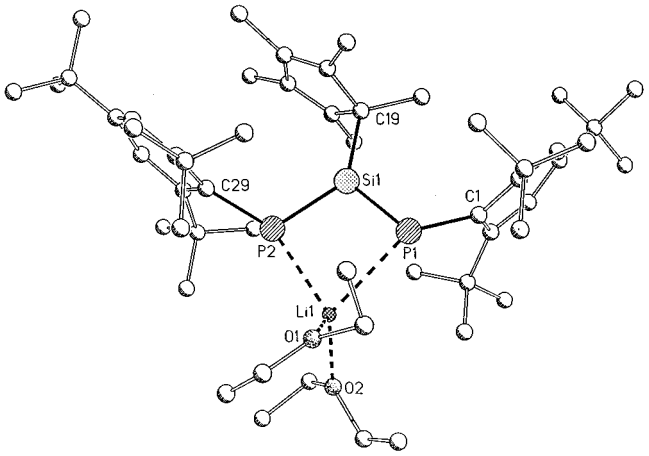

Figure 3. Molecular structure of the allylic complex **3c** ($2Et_2O$).

3a′ and **B**. In contrast, the compounds **3a**(**b**,**c**) and **A** reveal a remarkable distortion of the aryl ligands, resulting in dihedral angles for **3a** (CPPC) = 75.5° and **A** (CPPC) = 61.2°. This may be attributed to steric crowding of the system. However, the steric situation in the free anions, at least within the *E* half of the molecules, should be comparable. Hence, the main reason for the distortion seems to be the complexation

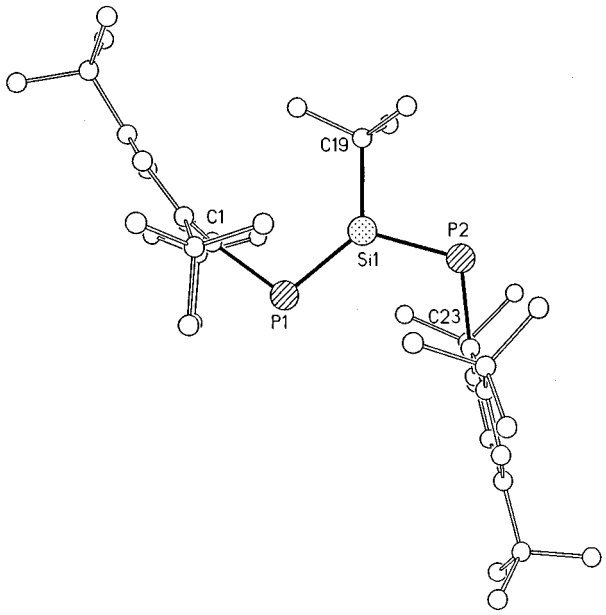

Figure 4. Molecular structure of the allylic anion **3a′**.

of the lithium by the two phosphorus atoms. The partly covalent P−Li bonding is indicated by the $^1J_{PLi}$ coupling in the ^{31}P NMR spectrum of **3a**. It induces a slight change in hybridization from sp^2 to sp^3 of the terminal atoms, which is in agreement with the observed differences in the ^{31}P NMR chemical shifts between **3a** and **3a′**.

Theoretical Procedure

Here we analyze the bonding in the lithium complexes. A second-order Jahn−Teller distortion of the planar complexes is evaluated. This induces a symmetry reduction from (C_{2v}) to (C_2) symmetry.

The analysis of bonding in the lithium compounds is based on the results of ab initio calculations of double-ζ quality. For this purpose, we performed quantum chemical calculations at the MP2(fc)/6-31+g(d) level. All were conducted with the GAUSSIAN 94 set of programs.[23,24] The stationary points on the electronic hypersurface were characterized with the corresponding vibrational analysis within the harmonic approximation, given the same computational level (MP2(fc)/6-31+g(d)) as in the structural optimizations. Additionaly, single-point calculations were performed at the optimized geometries, at a MP2 (fc)/6-311+g(d,p) triple ζ level. The details are given in the text.

(23) (a) Frisch, M. J.; Trucks, G. W.; Schlegel, H. B.; Gill, P. M. W.; Johnson, B. G.; Robb, M. A.; Cheeseman, J. R.; Keith, T.; Peterson, G. A.; Montgomery, J. A.; Raghavachari, K.; Al-Laham, M. A.; Zakrzewski, V. G.; Ortiz, J. V.; Foresman, J. B.; Cioslowski, J.; Stefanov, B. B.; Nanayakkara, A.; Challacombe, M.; Peng, C. Y.; Ayala, P. Y.; Chen, W.; Wong, M. W.; Andres, J. L.; Replogle, E. S.; Gomperts, R.; Martin, R. L.; Fox, D. J.; Binkley, J. S.; Defrees, D. J.; Baker, J.; Stewart, J. P.; Head-Gordon, M.; Gonzalez, C.; Pople, J. A. *Gaussian 94, Revision D.4*; Gaussian, Inc.: Pittsburgh, PA, 1995. (b) The refined 6-31+g(d) basis set was used (Gordon, M. S. *Chem. Phys. Lett.* **1980**, *76*, 163−168). The extended basis set (6-311g+(d,p) was taken from the work of Pople et al. (Krishnan, R.; Binkley, J. S.; Seeger, R.; Pople, J. A. *J. Chem. Phys.* **1980**, *72*, 650−654). The polarization functions were chosen according to the recommendations implemented in the Gaussian program, and the diffuse functions were chosen from Clark et al. (Clark, T.; Chandrasekhar, J.; Spitznagel, G. W.; Schleyer, P. v. R. *J. Comput. Chem.* **1983**, *4*, 294).

(24) (a) Møller, C.; Plesset, M. S. *Phys. Rev.* **1934**, *46*, 618. (b) Krishnan, R.; Pople, J. A. *Int. J. Quantum Chem.* **1978**, *14*, 91.

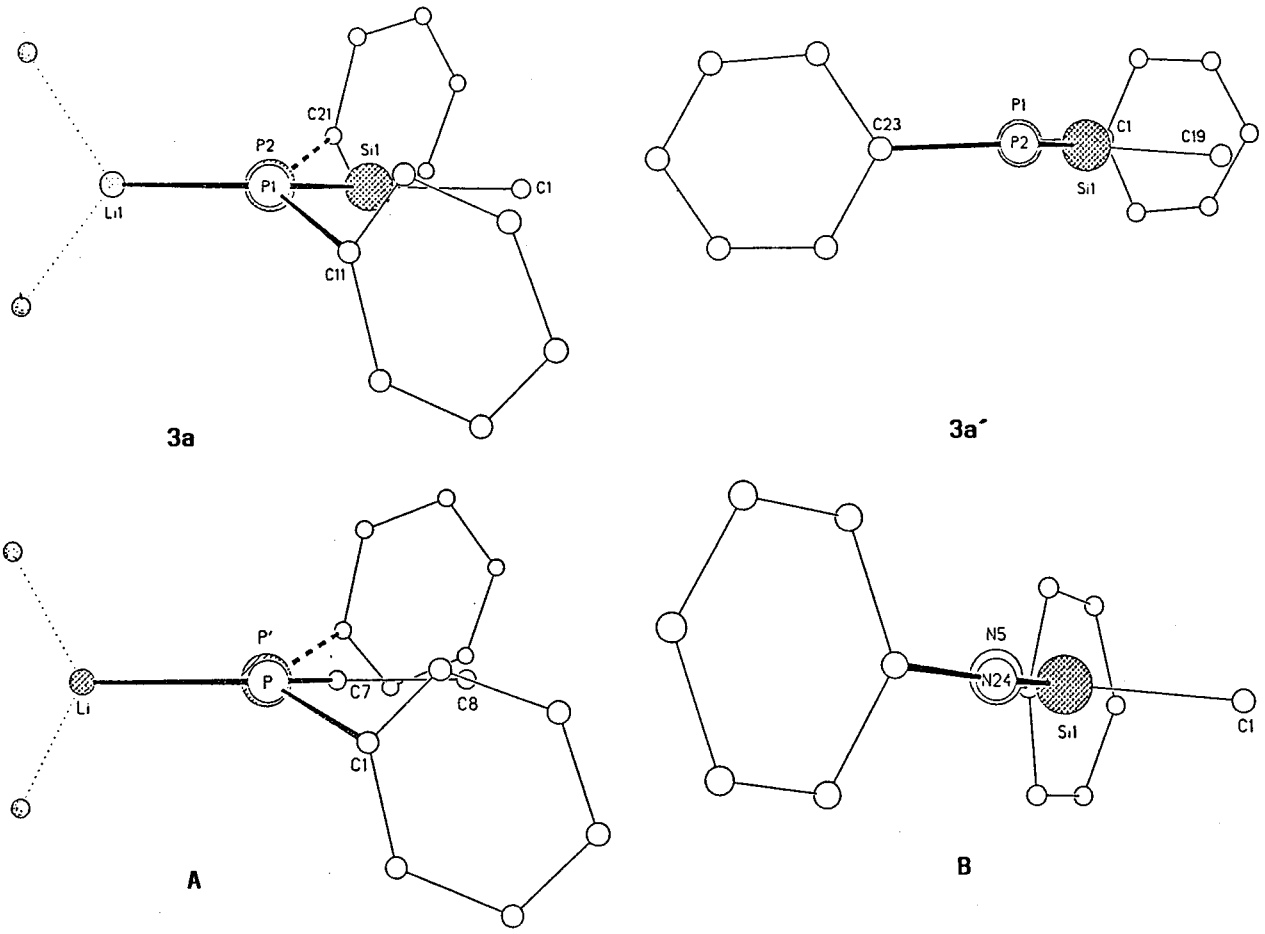

Figure 5. Newman plots along the P−P (N−N) axes of **3a** and **3a′**, as well as **A** and **B**.

MO Considerations. First we will analyze the qualitative aspects of the bonding situation in the parent Li complex of the allylic system. An interaction diagram for its composition is shown in Figure 6. It is logical to assume the composition of these adducts as a complex of an allylic anion with a lithium cation. The relevant orbitals of the allylic system (fragment A) are π_1 to π_3 and the positive (n_+) and the negative (n_-) combinations of lone pairs at the phosphorus atoms. These mingle with the (empty) s orbital (fragment B) of the lithium atom. Within C_{2v} symmetry (which imposes a planar geometrical arrangement), interaction between the a_1 orbital occurs resulting in C (C = A − B). However, bonding of the lithium to the allylic system requires a valence angle PSiP compression. Thus, in comparison with the free allylic system, the bonding (antibonding) orbitals n_+, π_1, and π_3 are lowered and n_- and π_2 are raised in energy, via through-space interaction. The qualitative nature of the orbital interaction diagram (Figure 6) is in conformity with the results of the ab initio calculations. As a result of (a) the weak (subfrontier orbital) interaction of the s orbital (fragment B) with n_+ and (b) valence angle compression PSiP, the frontier orbitals a_2 (HOMO), a_1, and b_1 (LUMO) come close to each other. As a consequence of this narrowing of the frontier orbitals, a second-order Jahn−Teller interaction becomes operative,[25] inducing symmetry reduction to C_2 or C_s symmetry,[26] as shown in Scheme 4.

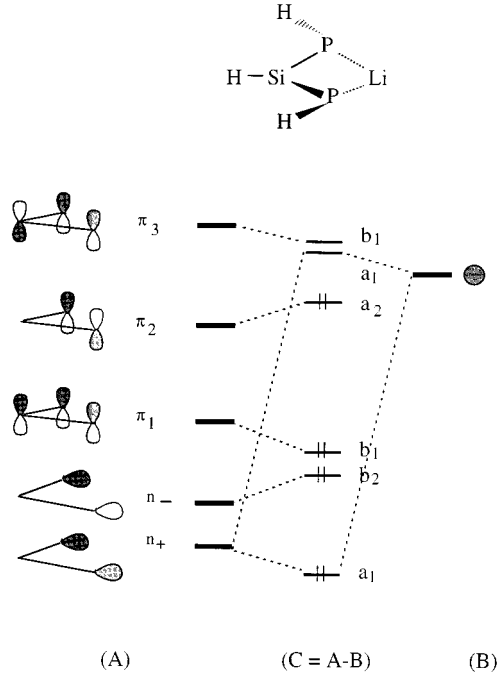

Figure 6. Interaction diagram for the formation of the Li complex (C = A − B) from the allylic fragment (A) with a Li atom (B).

(25) Pearson, R. G. *Symmetry Rules for Chemical Reactions*; Wiley: New York, 1976.

(26) Schoeller, W. W.; Niemann, J. *J. Am. Chem. Soc.* **1986**, *108*, 22−26.

Table 5. Crystallographic Data and Summary of Data Collection and Refinement[a]

	3a′	3b	3c
formula	$[C_{40}H_{67}P_2Si]^-[C_{20}H_{40}O_{10}Li_2Cl]^+ \cdot C_7H_8$	$[C_{45}H_{69}P_2Si]^-[C_4H_{10}O_2Li]^+ (C_4H_{10})$	$[C_{46}H_{73}P_2Si]^-[C_8H_{20}O_2Li]^+$
fw	1219.9	855.2	871.3
cryst syst	monoclinic	monoclinic	triclinic
space group	$P2_1/c$ (No. 14)	$C2/c$ (No. 15)	$P\bar{1}$ (No. 2)
cryst dimens, mm	0.3 × 0.4 × 0.4	0.5 × 0.6 × 0.7	0.9 × 0.9 × 0.9
cryst color	red	red	red
temp, K	193	293	293
a, Å	15.403(2)	24.636(5)	12.436(2)
b, Å	25.337(2)	15.852(3)	14.703(3)
c, Å	19.214(3)	18.025(3)	15.752(3)
α, deg			91.05(1)
β, deg	101.04(1)	124.20(1)	95.95(1)
γ, deg			93.66(1)
V, Å^3	7360	5822	2858
Z	4	4	2
ρ_{calc}, g cm^{-3}	1.10	0.98	1.01
radiation	Cu Kα	Mo Kα	Mo Kα
λ, Å	1.5418	0.7107	0.7107
μ, mm^{-1}	1.42	0.12	0.13
F (000)	2656	1880	960
max 2θ, deg	120	50	50
no. of variables	701	287	541
no. of reflns collcd	11 781	5332	10 188
no. of unique data	10 917	4970	9802
no. of data used in refinement ($\|F\| > 4\sigma(F)$)	8905	3005	7556
R	0.086	0.093	0.066
R_w	0.098	0.089	0.072
g	0.0005	0.0	0.0010
largest feature in final difference map, e Å^3	1.19 (in toluene)	0.42	0.81

[a] $R = \sum||F_o| - |F_c||/\sum|F_o|$ and $R_w = \sum(|F_o| - |F_c|)w^{1/2}/\sum|F_o|w^{1/2}$ with weighting scheme $w^{-1} = \sigma^2(F) + gF^2$.

To put the discussion on firmer ground, we performed ab initio calculations at the MP2(fc)/6-31+g(d) level on the parent structure **7**, imposing various possible symmetry constraints. The results of the investigations are summarized in Figures 7 and 8 and Table 6.

For completeness, we also included the free anions of the allylic systems under consideration in our treatment. At all levels of sophistication, the *Z*/*Z* conformation is the most stable, as compared with its *E*/*E* conformation. The *E*/*Z* conformation is intermediate in stability. The resulting energy differences (in kcal/mol) are at the MP2(fc)/6-311+g(d,p)//MP2(fc)/6-31+g(d) level (*Z*/*Z* 0.0; *E*/*Z* 1.6; *E*/*E* 3.1). The allylic anion is valence isoelectronic to the bis(imino)phosphorane, which also is known to preferentially adopt the *Z*/*Z* conformation.[27]

According to a vibrational analysis (within the harmonic approximation), the free anions adopt C_{2v} symmetry in their equilibrium structures. In contrast, the Li complex **7** results as a second-order saddle point on the electronic hypersurface. It possesses two imaginary frequencies (i475, a_2; i313, b_1, cm^{-1}). A C_2- or C_s-distorted geometry is lower in energy than the C_{2v} geometry. A corresponding vibrational analysis of these latter geometries reveals only the C_s- and C_2-symmetric structures as energy minima.

Noticeably, the resulting P−Li distances are shorter than those observed by the experiment. The calculated values are approximately 2.5 Å, while the experimental ones are approximately 2.6 Å. To examine the effect of solvation on the experimentally preferred C_s- or C_2-symmetric structures, we have surrounded **7** (C_2, C_s) by two water molecules and reoptimized the structures at the given computational level (MP/6-31+g(d)). The resulting relevant structural parameters are given in Figure 7 in parentheses. They differ to some extent from the unsolvated Li structures in that the P−Li distances increase to approximately 2.6 Å while the P−Si bonds are only slightly affected. Similarly, solvation only slightly increases the PSiP angle (in com-

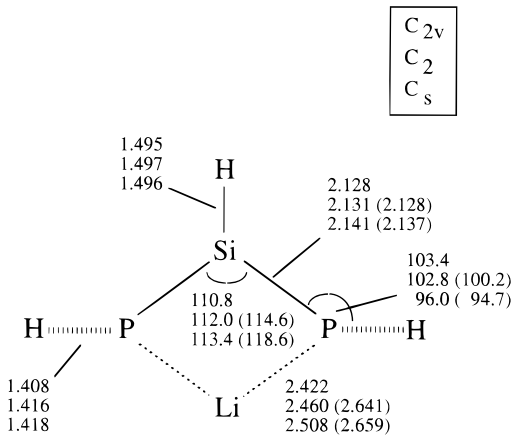

⊖ H(P)PSiP 180.0 (C_{2v})
141.0 (151.7) (C_2)
161.9 (166.8) (C_s)

⊖ H(Si)SiPP 171.4 (170.7) (C_s)

Figure 7. Bonding parameters (bond lengths in angstroms, bond angles in degrees) for **7** in C_{2v} (first entry), C_2 (second entry), and C_s symmetry (third entry). Relevant bonding parameters for solvated structures are given in parentheses.

(27) Schoeller, W. W.; Lerch, C. *Inorg. Chem.* **1986**, *25*, 576−580.

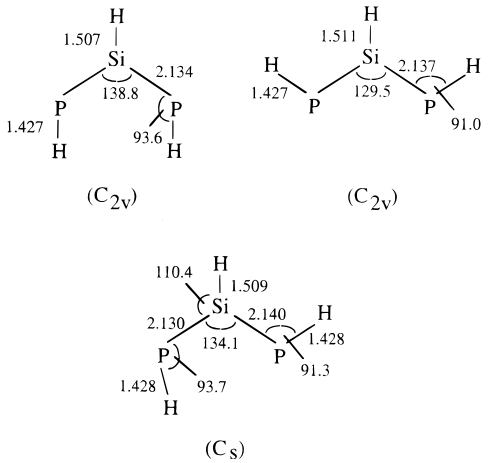

Figure 8. Bonding parameters (bond lengths in angstroms, bond angles in degrees) of the free parent allylic anions.

Table 6. Relative Energies (in kcal/mol) for 7 at Various Levels of Sophistication

symmetry	DZP[a]	DZP+ZPE[b]	TZP[c]
C_{2v}	0	0	0
C_2	−6.0	−5.3	−6.5
C_s	−10.0	−9.0	−11.0

[a] MP2(fc)/6-31+g(d) level. [b] Level *a* + ZPE vibrational correction (same level). [c] MP2(fc)/6-311+g(d,p) level//MP2(fc)/6-31+g(d) level.

parison with the unsolvated, gas-phase structures). According to the calculations, the C_s-symmetric structure is still 3.4 kcal/mol more stable than the C_2-symmetric structures (MP2/6-31+g(d)).

It must be noted that the considerations regarding solvation possess strong model character. In practice, the Li atom in the complex is surrounded by more sterically demanding ether molecules. In particular, only **3b** (see Table 4) strictly adopts C_2 symmetry; **3a** and **3c** reveal structures with two different P−Li bond lengths. In accordance with the theoretical analysis, it reveals the importance of an easy distortion from ideal C_2 symmetry. The C_s-symmetric alternatives, which are predicted as the lowest energy structural alternatives, are not observed, probably as a consequence of the larger steric demand of the bulky substituents attached to the phosphorus atoms. Within a C_s-symmetric arrangement, this would require a cis orientation of the substituents rather than a less sterically hindered trans geometry for the C_2-symmetric arrangement structures.

Experimental Section

^{31}P, ^{29}Si, ^{13}C, and ^{1}H NMR were determined on a Bruker AMX-300 (121.50, 59.25, 75.47, and 300.00 MHz) spectrometer. ^{7}Li NMR were recorded on a Varian FT-80A (30.91 MHz) instrument (1.5 M LiBr external reference). Mass spectra were measured on Masslab VG 12-250, Kratos MS-50, and Kratos Concept 1-H instruments. All reactions were carried out under an argon atmosphere in oven- or flame-dried glassware. The solvents used were dried by distillation from Na or Na/K. The silicon tetrachloride was dried by distillation from Al_2O_3. The (2,4,6-tri-*tert*-butylphenyl)phosphine was synthesized via the route described by Yoshifuji et al.[28]

(28) Yoshifuji, M.; Shima, L.; Inamoto, N. *J. Am. Chem. Soc.* **1983**, *105*, 2495.

Lithium 1,3-Bis[(2′,4′,6′-tri-*tert*-butylphenyl)phospha]-2-silaallylic Complexes (3a−f). (2,4,6-Tri-*tert*-butylphenyl)-phosphine (5.56 g, 20 mmol) was dissolved in 25 mL of dry diethyl ether and treated with *n*-BuLi (12.5 mL of a 15% solution in *n*-hexane). The resulting solution of **1** was stirred for 1 h and then cooled to −78 °C (MeOH/CO_2). Then 5 mmol of the desired trichlorosilane **2a**−**f** in 15 mL of dry diethyl ether was added slowly to give a yellow solution, which changed color to dark-red when warmed to room temperature (**3e** begins to decompose at −30 °C changing color to light green-yellow). All solvent was removed in vacuo and replaced by *n*-pentane before separation of the salts. After evaporation of the solvent, **3a**−**f** were obtained as sticky red-orange solids. Recrystallization from Et_2O/*n*-pentane or DME/*n*-pentane yielded dark red crystals of **3a** (2.46 g, 77%), **3b** (2.31 g, 58%), **3c** (2.65 g, 61%), and **3d** (2.11 g, 45%).

3a:[2] ^{31}P NMR (C_6D_6/Et_2O) δ −45.1 (q, J_{PLi} = 46.5 Hz, J_{PSi} = 145.2 Hz). ^{7}Li NMR (C_6D_6/Et_2O) δ +2.66 (t, J_{PLi} = 46.5 Hz). MS (15 eV) *m/e* 638 (M^+ − 2Et_2O − Li + H, 15). **3b**: ^{31}P NMR (C_6D_6/Et_2O) δ −33.3 (q, J_{PLi} = 47.9 Hz). ^{7}Li NMR (C_6D_6/Et_2O) δ −1.05 (t, J_{PLi} = 47.9 Hz). MS (15 eV) *m/e* 700 (M^+ − DME − Li + H, 11). **3c**: ^{31}P NMR (C_6D_6/Et_2O) δ −40.1 (s). ^{7}Li NMR (C_6D_6/Et_2O) δ −2.55 (s). MS (45 eV) *m/e* 722 (M^+ − 2Et_2O, 12), 716 (M^+ − 2Et_2O − Li + H, 42). **3d**: ^{31}P NMR (C_6D_6/Et_2O) δ −31.0 (s). ^{7}Li NMR (C_6D_6/Et_2O) δ −2.06 (s). MS (15 eV) *m/e* 784 (M^+ − 2Et_2O − Li + H, 24). **3e**: ^{31}P NMR (C_6D_6/Et_2O) δ −51.8 (s). ^{7}Li NMR (C_6D_6/Et_2O) δ −2.63 (s). **3f**: ^{31}P NMR (C_6D_6/Et_2O) δ −99.7 (q, J_{PLi} = 53.5 Hz). ^{7}Li NMR (C_6D_6/Et_2O) δ −0.90 (t, J_{PLi} = 53.5 Hz). MS (15 eV) *m/e* 842 (M^+ − 2Et_2O − Li + H, 9).

Lithium 1,3-Bis[(2′,4′,6′-tri-*tert*-butylphenyl)phospha]-2-*tert*-butylsilaallyl (15-Crown-5) Etherate (3a′). A freshly prepared solution of **3a** (5 mmol) was treated with a solution of 1.10 g (5 mmol) of 15-crown-5 in 10 mL of dry diethyl ether. After 1 h of stirring, all solvent was removed and replaced by *n*-pentane before the salts were separated. Again, the solvent was evaporated from the filtrate, and recrystallization of the residue from toluene yielded red crystals of **3a′** (2.38 g, 39%).

3a′: ^{31}P NMR (C_6D_6/Et_2O/−30 °C) (*E*/*E*) δ −22.3 (s, J_{PSi} = 183.1 Hz); (*E*/*Z*) δE −19.1 (d, J_{PP} = 30.5 Hz, J_{PSi} = 173.7 Hz), δZ −11.4 (d, J_{PP} = 30.5 Hz, J_{PSi} = 234.8 Hz).

1,3-Bis[(2′,4′,6′-tri-*tert*-butylphenyl)phospha]-2-silapropenes-(1) (4a−d). The solutions of **3a**−**d** in dry diethyl ether were treated with small amounts of wet diethyl ether at 0 °C, yielding the very unstable phosphinosilaphosphenes **4a**−**d**.

4a: ^{31}P NMR (C_6D_6/Et_2O) δP1 +142.0 (d, J_{PP} = 6.0 Hz, J_{P1Si} = 216.0 Hz); δP2 −125.0 (dd, J_{PP} = 6.0 Hz, J_{PH} = 206.2 Hz, J_{P2Si} = 95.2 Hz). **4b**: ^{31}P NMR (C_6D_6/Et_2O) δP1 +159.0 (d, J_{PP} = 14.6 Hz); δP2 −110.3 (dd, J_{PP} = 14.6 Hz, J_{PH} = 208.1 Hz). **4c**: ^{31}P NMR (C_6D_6/Et_2O) δP1 +169.2 (d, J_{PP} = 22.9 Hz); δP2 −124.0 (dd, J_{PP} = 22.9 Hz, J_{PH} = 210.8 Hz). ^{29}Si NMR (C_6D_6/Et_2O) δ +185.7 (dd, J_{P1Si} = 224.0 Hz, J_{P2Si} = 79.2 Hz). **4d**: ^{31}P NMR (C_6D_6/Et_2O) δP1 +163.8 (d, J_{PP} = 15.3 Hz, J_{P1Si} = 153.9 Hz); δP2 −101.7 (dd, J_{PP} = 15.3 Hz, J_{PH} = 238.1 Hz, J_{P2Si} = 134.8 Hz).

1,3-Bis[(2′,4′,6′-tri-*tert*-butylphenyl)phospha]-4-phospha-2-silabutenes-(1) (5a−e, 6a). A solution of 3 mmol of **3a** or **3b** in 20 mL of dry diethyl ether was cooled to −78 °C (MeOH/CO_2), mixed with a solution of 3 mmol of chlorophosphine **8a**−**e** in 5 mL of diethyl ether, and stirred for 2 h at this temperature. The color of the reaction mixture changed from dark red to orange. After the mixture was warmed to 25 °C, the solvent was removed in vacuo and dry *n*-pentane was added to the residue. The resulting solution was filtered, and the LiCl was washed several times with *n*-pentane. The filtrate was concentrated and allowed to crystallize at +4 °C. After 1 day, only the phosphasilene **5a**[17] was isolated as yellow crystals (1.41 g, 57%).

5a:[17] ^{31}P NMR (C_6D_6/Et_2O) δP1 +128.7 (dd, J_{P1P3} = 102.1 Hz, J_{P1P2} = 23.9 Hz); δP2 −69.1 (dd, J_{P2P3} = 215.2 Hz, J_{P2P1} =

23.9 Hz); δP3 −26.1 (dd, J_{P3P2} = 215.2 Hz, J_{P3P1} = 102.1 Hz). ^{29}Si NMR (C_6D_6/Et_2O) δ +180.2 (ddd, J_{P1Si} = 203.0 Hz, J_{P2Si} = 141.3 Hz, J_{P3Si} = 13.1 Hz). MS (15 eV) *m/e* 822 (M^+, 4), 277 ($C_{18}H_{30}P^+$, 100). **5b**: ^{31}P NMR (C_6D_6/Et_2O) δP1 +122.1 (dd, J_{P1P3} = 76.8 Hz, J_{P1P2} = 38.7 Hz); δP2 −75.8 (dd, J_{P2P3} = 315.8 Hz, J_{P2P1} = 38.7 Hz); δP3 +29.3 (dd, J_{P3P2} = 315.8 Hz, J_{P3P1} = 76.8 Hz). ^{29}Si NMR (C_6D_6/Et_2O) δ +185.9 (ddd, J_{P1Si} = 208.3 Hz, J_{P2Si} = 145.1 Hz, J_{P3Si} = 13.2 Hz). **5c**: ^{31}P NMR (C_6D_6/Et_2O) δP1 +107.7 (dd, J_{P1P3} = 75.9 Hz, J_{P1P2} = 42.9 Hz); δP2 −74.3 (dd, J_{P2P3} = 316.2 Hz, J_{P2P1} = 42.9 Hz); δP3 −2.8 (dd, J_{P3P2} = 316.2 Hz, J_{P3P1} = 75.9 Hz). ^{29}Si NMR (C_6D_6/Et_2O) δ +181.7 (ddd, J_{P1Si} = 200.8 Hz, J_{P2Si} = 138.4 Hz, J_{P3Si} = 4.9 Hz). **5d**: ^{31}P NMR (C_6D_6/Et_2O) δP1 +121.9 (dd, J_{P1P3} = 75.8 Hz, J_{P1P2} = 39.1 Hz); δP2 −75.7 (dd, J_{P2P3} = 317.3 Hz, J_{P2P1} = 39.1 Hz); δP3 +29.6 (dd, J_{P3P2} = 317.3 Hz, J_{P3P1} = 75.8 Hz). ^{29}Si NMR (C_6D_6/Et_2O) δ +186.0 (ddd, J_{P1Si} = 206.9 Hz, J_{P2Si} = 144.7 Hz, J_{P3Si} = 11.5 Hz). **5e**: ^{31}P NMR (C_6D_6/Et_2O) δP1 +114.9 (dd, J_{P1P3} = 101.2 Hz, J_{P1P2} = 34.8 Hz, J_{P1Si} = 207.4 Hz); δP2 −79.1 (dd, J_{P2P3} = 287.1 Hz, J_{P2P1} = 34.8 Hz, J_{P2Si} = 136.1 Hz); δP3 +12.0 (dd, J_{P3P2} = 287.1 Hz, J_{P3P1} = 101.2 Hz).

6a: ^{31}P NMR (C_6D_6/Et_2O) δP1 +157.7 (dd, J_{P1P2} = 44.1 Hz, J_{P1P3} = 9.0 Hz, J_{P1Si} = 197.0 Hz); δP2 −48.8 (dd, J_{P2P3} = 236.0 Hz, J_{P2P1} = 44.1 Hz, J_{P1Si} = 139.2 Hz); δP3 +0.2 (dd, J_{P3P2} = 236.0 Hz, J_{P3P1} = 9.0 Hz).

X-ray Structure Determination. X-ray Crystallographic Studies of 3a′, 3b, and 3c. X-ray data were collected with a Nicolet R3m (**3b**, **3b**) and Enraf-Nonius CAD4 (**3a′**) diffractometer by using the ω-scan technique. The structures were solved by direct methods. All non-hydrogen atoms were refined anisotropically (full-matrix least-squares on *F*; solvent in **3a′** and **3b** isotropically). H atoms were refined by using a riding model, and in **3b**, a *t*-Bu group was disordered (sof (C^{12}, C^{13}, C^{14}) = 0.54(3)). Calculations were performed using SHELXTL-Plus Inc., Madison, WI, 1989). Further details are given in Table 5.

Acknowledgment. We are grateful to the Fonds der Chemischen Industrie and the Studienstiftung des Deutschen Volkes for a scholarship (H.B.). We especially thank Prof. R. West, Prof. M. Koenig, Prof. J. Escudié, and Prof. M. Veith for the structural data of compounds **A** and **B**.

Supporting Information Available: Tables of the crystal structure details, atomic coordinates, bond lengths and angles, and hydrogen coordinates and ORTEP diagrams for **3a′**, **3b**, and **3c** (35 pages). Ordering information is given on any current masthead page.

OM9707937